Applied Thermal Engineering 238 (2024) 121950

Contents lists available at ScienceDirect

Applied Thermal Engineering

journal homepage: www.elsevier.com/locate/apthermeng

Research Paper

Evaluating the seawater desalination potential of an air-seawater system: through thermodynamic analysis and simulation of an indirect evaporative cooling desalination system

Hao Zhang, Xiaoyun Xie *

Building Energy Research Center, Department of Building Science, Tsinghua University, Beijing 100084, China

ARTICLE INFO

Keywords:
Desalination
Indirect evaporative cooling chiller
System exergy
Reversible transition
Seawater distribution ratio

ABSTRACT

This paper explores the desalination potential of a non-equilibrium air-seawater system. It provides calculations for thermodynamics at three different precision levels and introduces new insights, including the concept of system exergy and reversible transitions, to enhance the understanding of the evaporative cooling and desalination processes. The results indicate that for an air-seawater system at 30 °C, which includes 1 kg of dry air at a relative humidity of 45 % and 1 kg of seawater at a concentration of 3.5 %, there is a desalination potential of 0.138 kg of water product. Furthermore, a novel desalination process that utilizes an indirect evaporative cooling (IEC) chiller is designed, modeled, and simulated to estimate its freshwater production capacity. The simulation reveals a daily water product of 0.503 m^3 for specific 1 m^3*s^{-1} of air flow rate. A comprehensive sensitivity analysis of parameters is conducted based on this model. In comparison to the thermodynamic calculations, the simulated model exhibits a reversible efficiency of 3.6 % under typical conditions, suggesting there is ample room to further exploit the desalination potential of the non-equilibrium air-seawater system. Additionally, by incorporating comments on irreversible loss analysis, several optimized strategies are proposed. Considering the exergy inherent in non-equilibrium air-seawater systems is abundant, the concept of desalination based on non-equilibrium air-seawater system holds promise to yield economic benefits and reduce carbon emissions.

1. Introduction

Water shortage exists across each continent to varying degrees, and around 3.42 billion people are experiencing scarcity of fresh drinkable water [1]. Meanwhile 97 % of the water on earth is seawater [2], thus desalination by which fresh water is obtained from seawater is a feasible and promising way to alleviate water shortage. Conventional desalination technologies mainly include reverse osmosis (RO), multi-stage flash (MSF), multi-effect distillation (MED) which all feature in large-scale water supply and energy intensive, and need huge investment for continuous operation and routine maintenance [3]. Different from the MSF and MED processes, humidification-dehumidification (HDH) desalination is introduced and arouses attention of researchers, in which heat and mass transfer processes occurs in atmosphere environment instead of vacuum environment in MED and MSF.

A typical HDH system is shown in Fig. 1. It includes a humidifier, dehumidifier and a heater, which is usually a solar collector. The principle of HDH is similar to evaporation and rainfall in nature. The air circulates between humidifier and dehumidifier, and in dehumidifier, freshwater is condensed and collected. HDH is a thermal desalination method, which actually utilize the heat from the sun or elsewhere and seawater as cooling source. Unlike MSF and MED, HDH system doesn't need a vacuum operation condition, and the temperature could be lower, which results in lower gain output ratio. However, it has a lower investment and is suitable for small-scale water supply, especially with abundant solar energy resource [4].

For HDH system, when night or other situations without heat supply, the water product decreases significantly. For some particular HDH processes where air is in close-cycle and there is no fresh air inlet, no heat supply means zero exergy input and zero freshwater product. However, for a process where seawater and air are in open-cycle, the system itself has work potential, because non-saturated moist air and seawater are in non-equilibrium state. Thus, a non-equilibrium air-seawater system has desalination potential. On the other hand, a non-equilibrium air–water system is generally utilized in cooling system, which is called evaporative cooling. It is a simple idea that fresh water could be obtained by dehumidifying moist air using evaporative cooling resource.

* Corresponding author.
E-mail address: xiexiaoyun@tsinghua.edu.cn (X. Xie).

https://doi.org/10.1016/j.applthermaleng.2023.121950
Received 8 August 2023; Received in revised form 4 November 2023; Accepted 6 November 2023
Available online 10 November 2023

Nomenclature

Acronyms

DPD dew-point desalination
DWP daily water product for specific 1 m^3*s^{-1} of air flow rate [$m^3*d^{-1}*m^{-3}*s$]
GOR gain output ratio
HDH humidification-dehumidification desalination
HEX heat exchanger
HMX heat and mass exchanger
IEC indirect evaporative cooling
IWP ideal water product capacity for specific 1 kg of air [$kg*kg^{-1}$]
MED multi-effect distillation desalination
MSF multi-stage flash desalination
NTU number of transfer units
rh relative humidity
RIEC regenerative indirect evaporative cooling
RO reverse osmosis desalination
SDR seawater distribution ratio
SEC specific energy consumption for specific 1 m^3 of water product [$kWh*m^{-3}$]

Greek Symbols

ε heat transfer effectiveness
μ chemical potential [$kJ*kg^{-1}$]
ω humidity ratio [$kg*kg^{-1}$]

Roman Symbols

c specific heat capacity [$kJ*kg^{-1}*K^{-1}$]
E exergy [kJ]
e specific exergy [$kJ*kg^{-1}$]
G Gibbs free energy [kJ]
g specific Gibbs free energy [$kJ*kg^{-1}$]
H enthalpy [kJ]
h specific enthalpy [$kJ*kg^{-1}$]
M molar mass [$kg*kmol^{-1}$]
m mass [kg]
P pressure [kPa]
R gas constant [$kJ*kg^{-1}*K^{-1}$] [$kJ*kmol^{-1}*K^{-1}$]
S entropy [$kJ*K^{-1}$]
s specific entropy [$kJ*kg^{-1}*K^{-1}$]
T temperature [K] [°C]
W quantity of performing work [kJ]
w specific freshwater extracting energy [$kJ*kg^{-1}$]
x concentration of seawater

Subscripts

0 surroundings state or initial state
1,2,3 different calculation methods
a air
DA dry air
deh dehumidifier
E extracting energy
e equilibrium state
fw freshwater
h heat
m mass
p isobaric
s system
sat saturation state
sw seawater
v water vapor
w water
x concentration

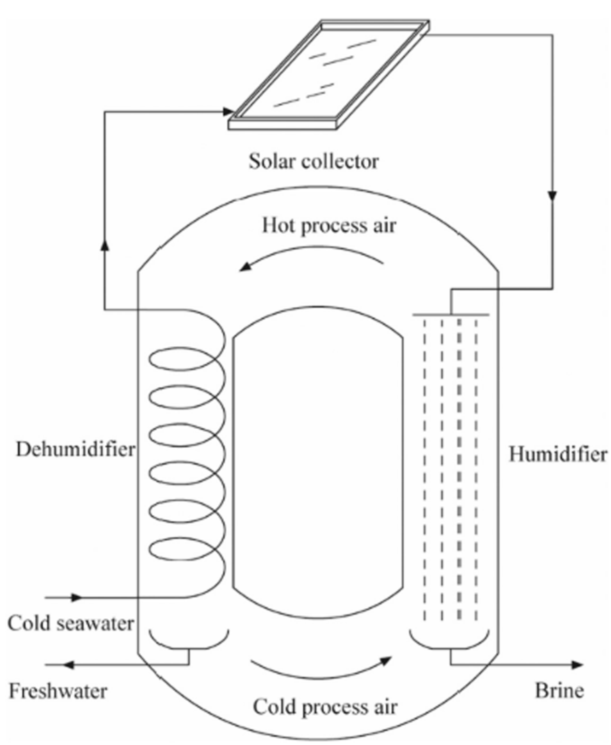

Fig. 1. Typical HDH system [4].

Evaporative cooling is widespread used to remove heat with water evaporation and has a variety of applications, from industrial to air conditioning systems [5]. Evaporative cooling has been developed for a long history. Indirect evaporative cooling (IEC), developed from conventional evaporative cooling technology, could achieve lower temperature, as low as the outdoor air dew point temperature, and has great potential in reducing energy consumption [6]. IEC has been regarded as one of the promising methods to substitute air conditioner, especially in arid regions [7]. IEC can produce cooling capacity with the lowest possible temperature, which is also needed for dehumidification in HDH.

In an IEC system, there exists an air cooler, where air doesn't contact water directly and there is only heat transfer and no mass transfer. In initial IEC, part of air participates evaporating and part of air is cooled down to supply to the room [8]. Now the IEC has been improved and can be classified into M−cycle, regenerative IEC (RIEC) and IEC chiller. M−cycle and RIEC are designed to obtain cooling air to the room and have been utilized in widespread air conditioning system [7,8,9]. IEC chiller is proposed by Jiang and Xie [10] to supply cooling water, which could be used in data center cooling, also in some air conditioning systems [11]. There have been a lot of literatures about comparison among these forms [12,13]. Different configurations of these forms are shown in Fig. 2. IEC technology could achieve lower temperature than environment air wet bulb by pre-cooling down the inlet air, and the theoretical limit of IEC could be the dew point, which expands the applicable regions[14].

In fact, there have been several researches conducted to explore the integration of HDH and IEC. Most of them focus on improving the water product of the HDH system by adding IEC sections. Kabeel et al. [15]

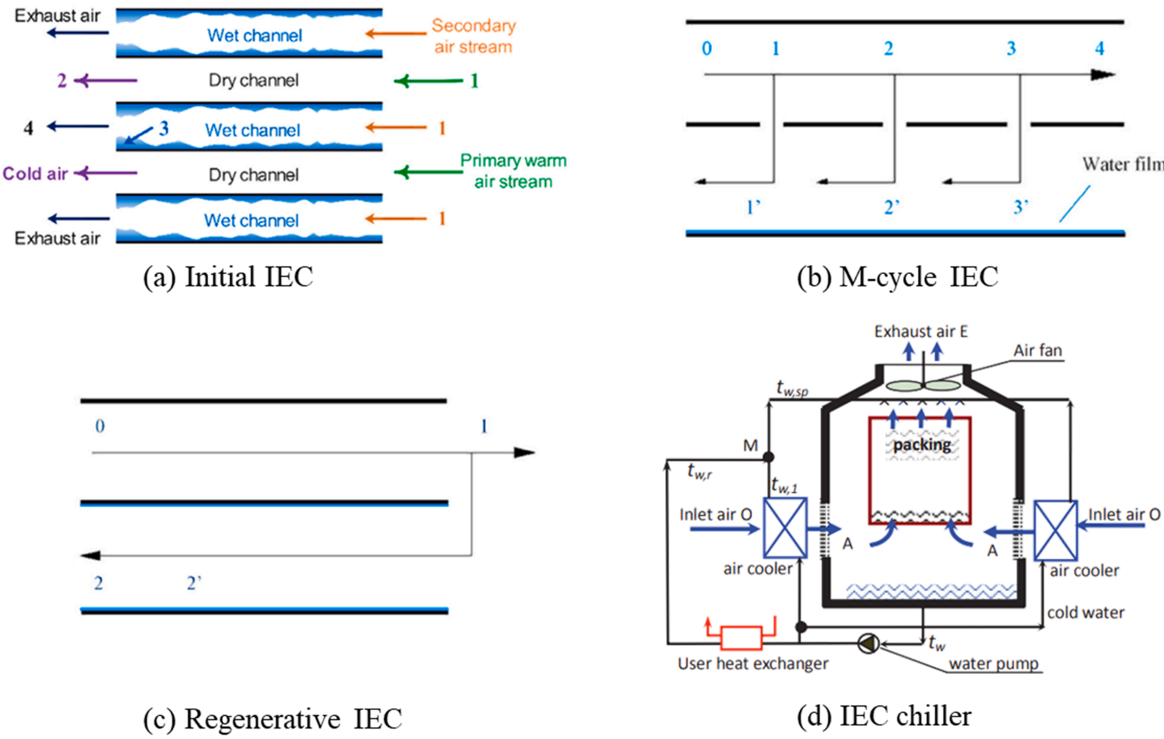

Fig. 2. Different types of IEC process [8,9,12].

designed and fabricated a hybrid system that combines a conventional IEC cooler and an HDH system to simultaneously produce cooling air and freshwater. Chen et al. [16] developed a hybrid system consisting of an RIEC cooler and an HDH system, also aiming to achieve simultaneous production of cooling air and freshwater. Tariq et al. [17] and Aziz et al. [18] proposed similar hybrid systems combining M−cycle or regenerative IEC with an HDH system to enhance water production capacity. Rocchetti and Socci [19] designed a hybrid system incorporating RIEC, compression heat pump, and HDH system to further increase water production. Very few studies address the desalination potential of the air-seawater system itself or the HDH system without a heat source. A related work, conducted by Pandelidis et al. [20]

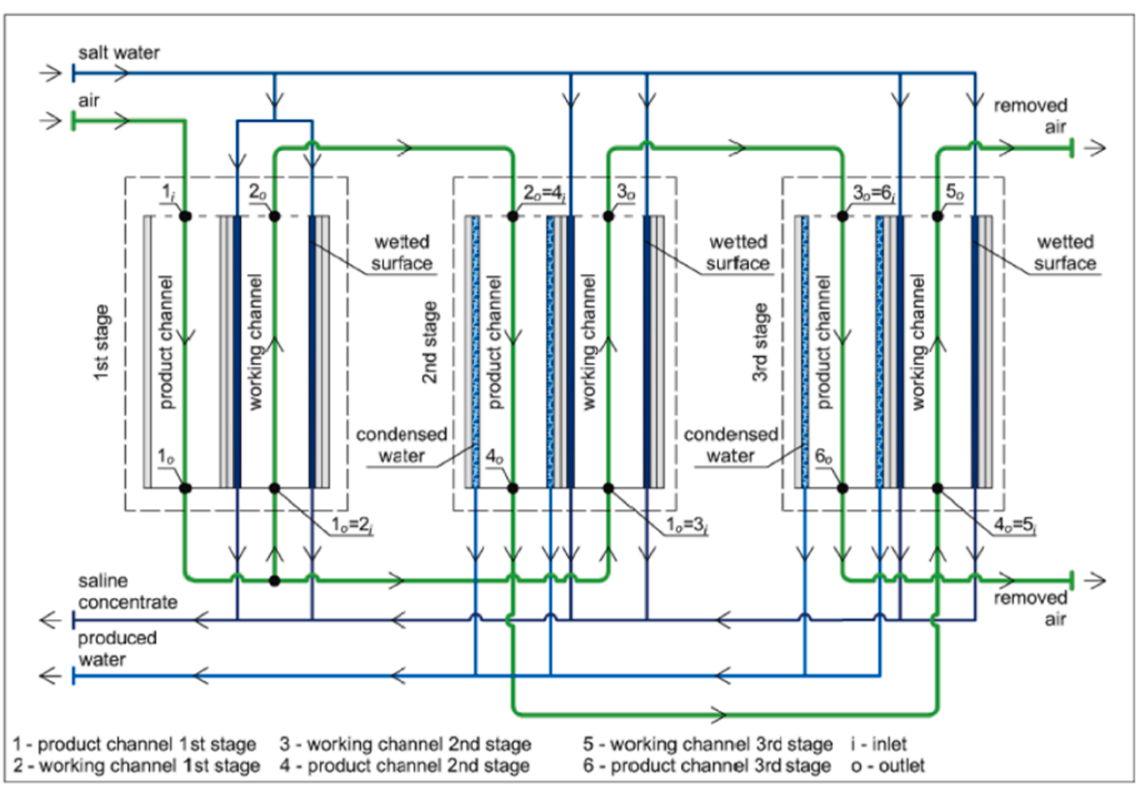

Fig. 3. Previous dew point desalination system [20].

proposed a desalination system based on a regenerative IEC system with several humidifier-dehumidifiers, as shown in Fig. 3, and conducted a sensitivity analysis for some parameters. However, no prior research has been conducted on the thermodynamic analysis of the work capacity and desalination potential of the air-seawater system. Moreover, there is a possibility for introducing new air-seawater desalination processes, and sensitivity studies on certain parameters need to be addressed comprehensively. Combining thermodynamic analysis with system design is not only beneficial but also essential.

To address the gap in thermodynamic analysis of the water production potential of air-seawater systems, this paper calculates the water production limits of air-seawater systems and introduces two useful thermodynamic calculation methods. Additionally, the paper presents the design and simulation of a novel air-seawater desalination process based on IEC chillers, which is more straightforward, and offers a sensitivity analysis of relevant parameters. Finally, several comments are given on economics analysis and irreversible loss. The exergy inherent in non-equilibrium air-seawater systems can be considered as both abundant and readily available and has been extensively utilized in the field of evaporative cooling. Applying this concept to seawater desalination holds promise as it has the potential to yield economic benefits and reduce carbon emissions. This is the primary objective of this paper, which aims to assess the desalination potential of air–water systems from both thermodynamic limits and practical process design perspectives.

2. Theoretical calculation of thermodynamic limit

In this section, the desalination potential of air-seawater system is calculated based on thermodynamics. Three theoretical calculation methods are introduced in different precision levels. Methods 2 and 3 have made significant advancements compared to conventional exergy analysis methods and may serve as a source of inspiration for similar problems in the field. All discussion is under environmental pressure, 101.3 kPa.

2.1. Moist air exergy and extracting energy of freshwater

The most common way to obtain the limit is to separately calculate the moist air exergy and extracting energy of freshwater from seawater. The exergy of moist air is depending on reference point and can be divided into heat exergy and mass exergy. For moist air whose temperature at T and humidity ratio at ω, the exergy of moist air can be divided into heat exergy e_h and mass exergy e_m [21] and calculated using formula (1) ~ (3) [22].

$$e = e_h + e_m \tag{1}$$

$$e_h = \left(c_{p,DA} + \omega c_{p,v}\right)\left(T - T_0 - T_0 \ln\frac{T}{T_0}\right) \tag{2}$$

$$e_m = T_0 R_a\left[(1 + 1.608\omega)\ln\left(\frac{1 + 1.608\omega_0}{1 + 1.608\omega}\right) + 1.608\omega \ln\frac{\omega}{\omega_0}\right] \tag{3}$$

Where T_0 and ω_0 represent the reference point. $c_{p,DA}$ and $c_{p,v}$ represent the specific isobaric heat capacity of dry air and vapor. R_a is the specific gas constant of air which is given by molar gas constant divided by the molar mass of air, which is equal to 0.287 $\mathrm{kJ{*}kg^{-1}{*}K^{-1}}$.

The reference point usually is at the saturated state related to water in a psychrometric diagram in a conventional evaporating cooling system. However, in our case, since the reference point depends on seawater, it is more appropriate to select the saturated state related to seawater as the reference point.

On the other hand, extracting energy of water from seawater is defined as the work needed to extract 1 kg water from an infinite amount of seawater at a given concentration x, and a certain temperature T_0. Extracting energy can be calculated with formula (4), where g_w and μ_w represent the specific Gibbs free energy of water and the chemical potential of water in seawater solution. Since the chemical potential is also the partial Gibbs free energy of water in seawater, which represents the Gibbs free energy of 1 kg water in infinite seawater solution at certain concentration, the difference of g_w and μ_w is equal to the minimal work needed to extract 1 kg water from seawater.

$$w_E = g_w - \mu_w \tag{4}$$

g_w is the property of pure water and easy to get based on Refprop database [23]. The chemical potential of water in seawater μ_w can be obtained based on seawater properties with formula (5). The enthalpy H_{sw} and entropy S_{sw} of seawater can be calculated using correlations given by Nayar, K. G., et al. [24]. The differentiation can be calculated using formula (6) with the help of software EES [25].

$$\mu_w = \overline{G}_w = \left(\frac{\partial G_{sw}}{\partial m_w}\right)_{T,P,x_0} = \left(\frac{\partial (H_{sw} - TS_{sw})}{\partial m_w}\right)_{T,P,x_0} \tag{5}$$

$$\mu_w = \lim_{m\to 0}\frac{(m_0+m)\left(h|_{x=\frac{x_0}{1+\frac{m}{m_0}}} - Ts|_{x=\frac{x_0}{1+\frac{m}{m_0}}}\right) - m_0\left(h_{x_0} - Ts_{x_0}\right)}{m} = \lim_{\frac{m}{m_0}\to 0}\frac{\left(1+\frac{m}{m_0}\right)\left(h|_{x=\frac{x_0}{1+\frac{m}{m_0}}} - Ts|_{x=\frac{x_0}{1+\frac{m}{m_0}}}\right) - \left(h_{x_0} - Ts_{x_0}\right)}{\frac{m}{m_0}} \tag{6}$$

By dividing the moist air exergy e by the extracting energy w_E, shown in formula (7), we can determine the theoretical limit of water production per 1 kg of dry air, which is called ideal water product capacity (IWP) here.

$$IWP_1 = \frac{e}{w_E} \tag{7}$$

2.2. Air-seawater system exergy and extracting energy

As introduced in 2.1, the exergy of moist air is depending on the reference point related to the seawater, which also indicates there is infinite seawater resources [26]. In most literature about the exergy analysis of thermal systems, such as nuclear/thermal power plant or chemical plant, the reference temperature is often selected as the temperature of air or seawater, corresponding to evaporative cooling or seawater cooling, and the selection of reference temperature also indicates the infinite cooling resource at this temperature. But in our study, the exergy is furtherly discussed under finite moist air and seawater, which is called system exergy E_s in this paper. System exergy indicates the maximum work capacity of an adiabatic non-equilibrium system, while it is obvious that an equilibrium system has no capacity of performing work outwards.

System exergy is different from the exergy in the usual sense, but the latter could be considered as the system exergy of a special system including the infinite environment resource selected as reference point, and therefore, the system exergy E_s is always smaller than the exergy E in the usual sense due to the inclusion of finite resources.

According to the definition of system exergy above, the system exergy of air-seawater system E_s (for specific 1 kg of dry air) achieves maximum e obtained in section 2.1 when there is infinite seawater. Now assume a system includes air and finite seawater, the system exergy, or the maximum work capacity E_s can be obtained with following ideas. Suppose the system keep exhibits outward work reversibly and adiabatic until it achieves an equilibrium state, the energy or the total enthalpy this system decreases due to the First law of thermodynamics. When the system reaches the equilibrium state, the quantity of work, which is also the system exergy E_s, is equal to the decrease in system enthalpy, represented by -ΔH. A flowchart illustrates these ideas in Fig. 4.

The E_s can be calculated with Fig. 4 and equations (8) ~ (13). Where the subscript e represents the equilibrium state also the final state. The M_{DA} and M_w represent the molar masses of dry air and water, respectively. $p_{sat,x}$ represents the partial saturation pressure of water corresponding to the seawater concentration. p_0 represents the atmosphere pressure, which is equal to 101.3 kPa.

$$m_e + \omega_e \cdot m_{DA} = m_0 + \omega_0 \cdot m_{DA} \qquad \textit{Mass Conservation} \tag{8}$$

$$m_e x_e = m_0 x_0 \qquad \textit{Solute Conservation} \tag{9}$$

$$T_{a,e} = T_{sw,e} \qquad \textit{Temperature Equilibrium} \tag{10}$$

$$p_{sat,x_e} = \frac{\frac{m_{DA}\omega_e}{M_w}}{\frac{m_{DA}}{M_{DA}} + \frac{m_{DA}\omega_e}{M_w}} \cdot p_0 \qquad \textit{Phase Equilibrium} \tag{11}$$

$$\Delta S = 0 \qquad \textit{Zero Entropy Generation} \tag{12}$$

$$E_s = -\Delta H \qquad \textit{Energy Conservation} \tag{13}$$

The specific realization of the work process is irrelevant, because the limit problem is more concerned here. But for ease of understanding, a system composed of reversible turbine, water molecule semipermeable membranes, heat engine, piston and other components can be imagined as shown in Fig. 5. In this ideal system, the turbine between two water molecule semipermeable membranes is driven by the water partial pressure difference of two sides to perform work. The seawater temperature decreases due to the evaporation of water, causing temperature difference between the air and seawater. Thus, a heat engine could exhibit outward work, which absorbs heat from the air and releases heat to the seawater to maintain the temperature equilibrium. Besides, due to the phase transition of water, and the temperature change of air, the volume of this system tends to change and the piston moves, resulting in the pressure–volume work, which is equal to 0 because the system and the surrounding have no pressure difference. E_s is aggregate of the turbine work and heat engine work when the system is from initial state to equilibrium state. The system exergy can be seen as an analogous concept to the free energy change under adiabatic and isobaric conditions, although it is discussed less frequently in this manner.

Once E_s is obtained, divide it by the extracting energy w_E calculated in 2.1, a more accurate theoretical limit of water product IWP_2 could be obtained using formula (14). This method actually describes a more accurate system exergy, under the condition of finite seawater.

$$IWP_2 = \frac{E_s}{m_{DA} w_E} \tag{14}$$

2.3. Reversible adiabatic transition

Method 2 cannot accurately calculate the theoretical water production limit under finite seawater conditions, due to the variation in extracting energy w_E caused by the increase in seawater concentration at the outlet. Besides, solution mixing heat impact is not taken into consideration, although it is very slight in this case. However, there is a direct method to calculate the water product limit. Like 2.2, considering an adiabatic and reversibly process, but the air-seawater system does not perform work on the surroundings. Instead suppose some kind of reversible transition occurs inside the system, fresh water is directly separated. When the air, seawater and freshwater achieve the temperature equilibrium, also the air and seawater achieve phase equilibrium, the freshwater product reaches its maximum.

Following similar principles as in Section 2.2, the calculation process is shown in Fig. 6 and equation (15) ~ (20). It has to be mentioned that although the equations here are similar to those in 2.2, the method 3 here actually assumes a reversible desalination process. It is different from the method 2, which is still from the perspective of exergy, like the method 1.

$$m_e + \omega_e \cdot m_{DA} + m_{fw} = m_0 + \omega_0 \cdot m_{DA} \qquad \textit{Mass Conservation} \tag{15}$$

$$m_e x_e = m_0 x_0 \qquad \textit{Solute Conservation} \tag{16}$$

$$T_{a,e} = T_{sw,e} = T_{fw,e} \qquad \textit{Temperature Equilibrium} \tag{17}$$

$$p_{sat,x_e} = \frac{\frac{m_{DA}\omega_e}{M_w}}{\frac{m_{DA}}{M_{DA}} + \frac{m_{DA}\omega_e}{M_w}} \cdot p_0 \qquad \textit{Air - seawater Phase Equilibrium} \tag{18}$$

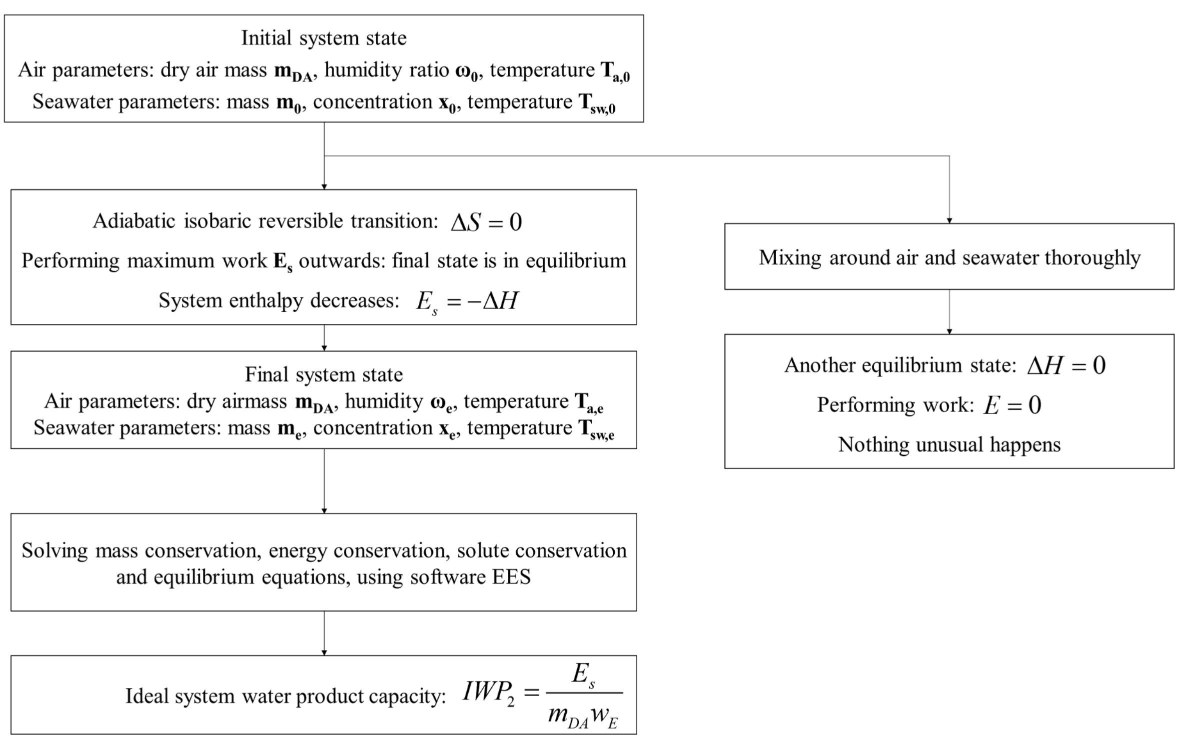

Fig. 4. Adiabatic and reversible performing work process calculation flowchart.

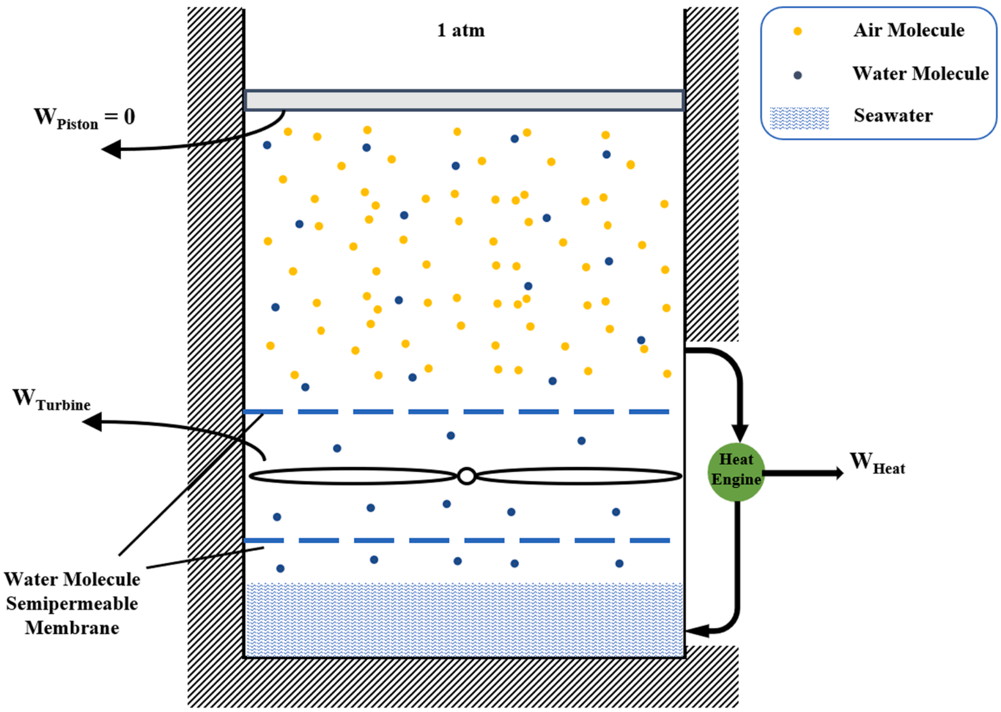

Fig. 5. An ideal work diagram of air-seawater system.

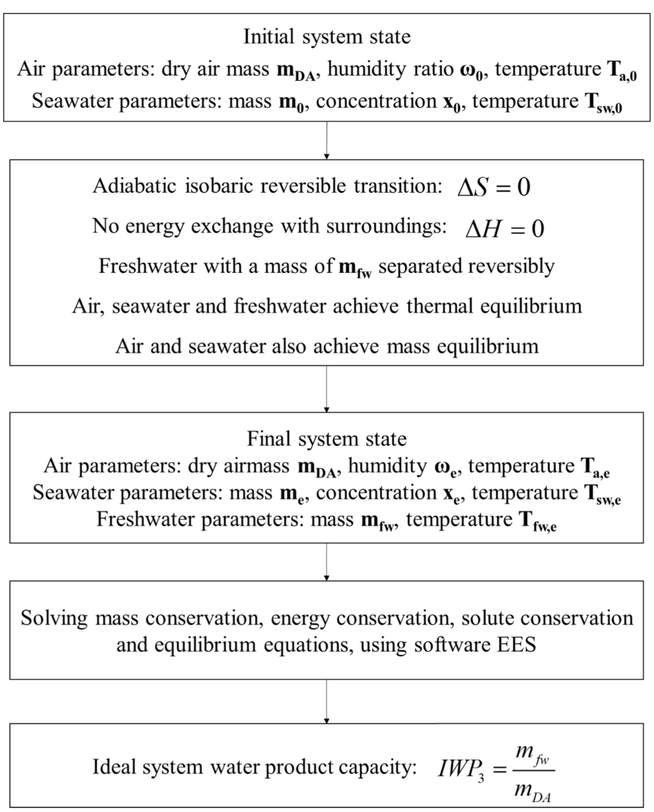

Fig. 6. Adiabatic and reversible desalination transition process calculation flowchart.

$$\Delta S = 0 \qquad \textit{Zero Entropy Generation} \tag{19}$$

$$\Delta H = 0 \qquad \textit{Energy Conservation} \tag{20}$$

The ideal water product capacity can be obtained with formula (21). This method does not rely on the exergy or extracting energy and provides the most accurate thermodynamic limit of water product capacity for an air-seawater system.

$$IWP_3 = \frac{m_{fw}}{m_{DA}} \tag{21}$$

2.4. Conclusions of three methods

The results based on three methods are calculated using software EES. For 1 kg of dry air at a temperature of 30 °C, a relative humidity of 45 %, and varying masses of seawater at a concentration of 3.5 % and a temperature of 30 °C, the results for exergy (or system exergy), extracting energy and theoretical water product capacity are presented in Table 1.

According to Table 1, the ideal water product capacity calculated using Method 1 is significantly greater than that of Method 2, 3. And under the same seawater and air mass ratio, the ideal water product

Table 1
Comparison of results based on three methods.

	Extracting energy	Seawater mass	Exergy (or system exergy)	Ideal water product capacity
Method 1	2.76 kJ/kg	–	0.694 kJ	0.251 kg*kg^{-1}
Method 2	2.76 kJ/kg	0.5 kg	0.344 kJ	0.125 kg*kg^{-1}
		1.0 kg	0.419 kJ	0.152 kg*kg^{-1}
		2.0 kg	0.496 kJ	0.180 kg*kg^{-1}
		5.0 kg	0.576 kJ	0.209 kg*kg^{-1}
Method 3	–	0.5 kg	–	0.107 kg*kg^{-1}
		1.0 kg	–	0.138 kg*kg^{-1}
		2.0 kg	–	0.170 kg*kg^{-1}
		5.0 kg	–	0.203 kg*kg^{-1}

capacity calculated using Method 3 is slightly lower than that obtained using Method 2. These results are as expected since, as mentioned before, Method 2 and Method 3 respectively take into account the finite seawater case, with Method 3 providing a more comprehensive consideration. Theoretically, when the seawater and air mass ratio achieve infinite, the result of three methods will achieve the same.

Since Method 3 provides the most precision level, using Method 3, ideal water product capacity is examined under various conditions. Under typical condition where mass ratio of seawater to dry air is 1.0, inlet temperature of air and seawater is 30 °C, relative humidity of inlet air is 45 %, the concentration of seawater is 3.5 %, the parameters sensitivities are shown in Fig. 7. In each diagram of Fig. 7 (a)~(d), only the parameter in horizontal axis is changed. The vertical axis represents the ideal water product capacity for specific 1 kg of dry air, with a unit of [kg*kg^{-1}]. According to Fig. 7, ideal water product capacity increases when the mass ratio of seawater to air increases, but has a limit. Besides, ideal water product capacity increases when inlet temperature increases, relative humidity of inlet air decreases and the concentration of seawater decreases.

Based on the results, for 1 kg of dry air with a relative humidity of 45 % and 1 kg of seawater in the system at 30 °C, the potential water production capacity is 0.138 kg. This is a significant finding; however, it can only be achieved under reversible conditions. Therefore, an air-seawater desalination system based on IEC chiller is subsequently designed, modeled, and simulated to evaluate the practical performance of this concept.

3. Design, modelling and simulation of an IEC chiller desalination system

3.1. Process design and modelling

In this section, a simple desalination system is designed and a numerical model is established. This system is based on an IEC chiller system, with two heat exchangers (HEX) and a heat and mass exchanger (HMX). Two heat exchangers are separately dehumidifier and pre-cooler. The heat and mass exchanger, which is actually a padding tower, is used as a humidifier.

The process is shown in Fig. 8. In pre-cooler, the air is cooled by one branch of chilled seawater from padding tower firstly, and the enthalpy or the wet bulb temperature of air decreases, which help to product lower temperature of seawater in padding tower. Padding tower is the place where heat and mass transfer occurs between air and seawater, which is one of the most common type of evaporative cooling tower. In dehumidifier, the chilled seawater from padding tower dehumidifies the moist air from padding tower. In all three components, the heat and mass transfer processes between air and seawater are counter-flow. The inlet air goes through pre-cooler, padding tower and dehumidifier sequentially, while the inlet seawater goes through padding tower first, and then is divided into two streams which separately go into the pre-cooler and dehumidifier.

The principle is simple as well. The pre-cooler and padding tower constitute an IEC water chiller system, which could obtain chilled water with a temperature limit at the dew point of the inlet air. Then use the chilled water to dehumidify the outlet air of padding tower, and the freshwater could be obtained.

A numerical model is established, based on the following assumptions:

(1) Each process is considered as a whole part calculated by the effectiveness ε of HEX or HMX which is given;
(2) The moist air leaves the padding tower and dehumidifier with a relative humidity of 100 % [16];
(3) The system has achieved a steady state;
(4) The properties of seawater are calculated using correlations developed by Nayar [24]. The air is considered as ideal gas mixture consisting of steam and dry air;

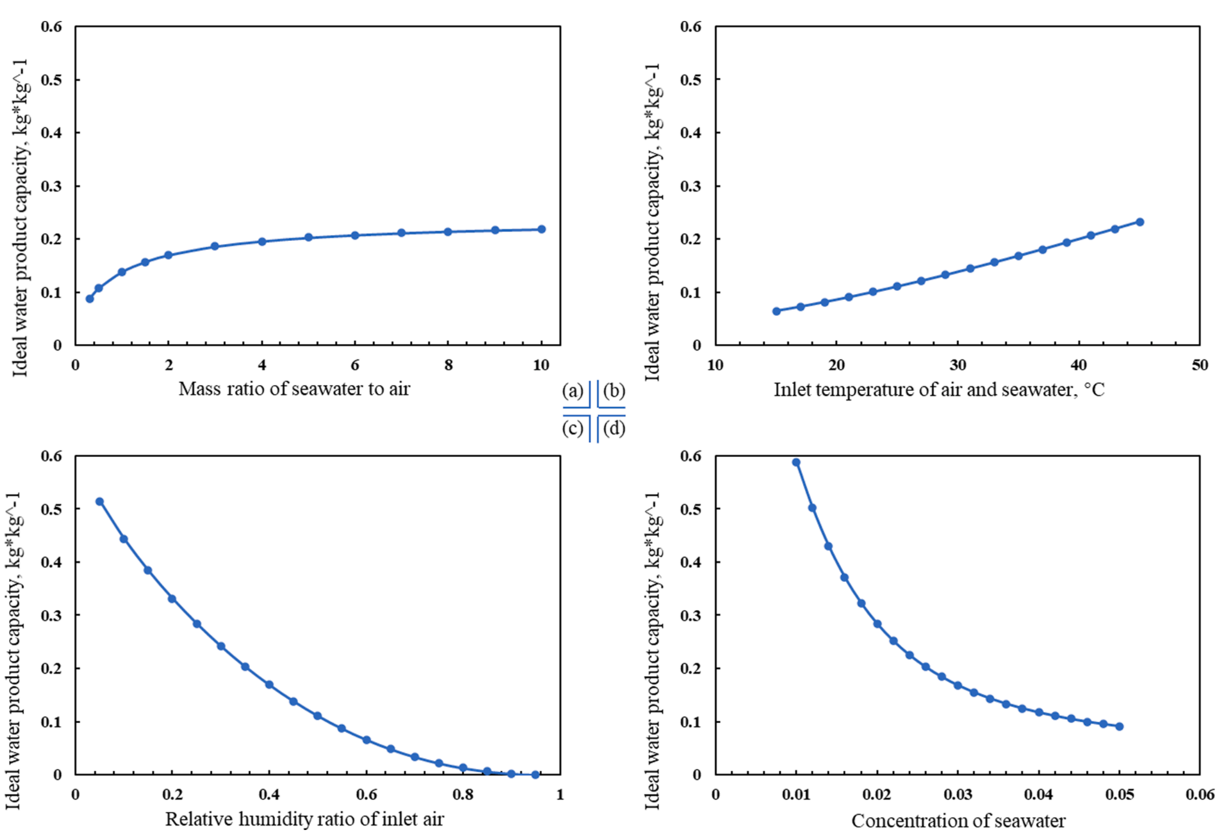

Fig. 7. Ideal water product capacity under different conditions.

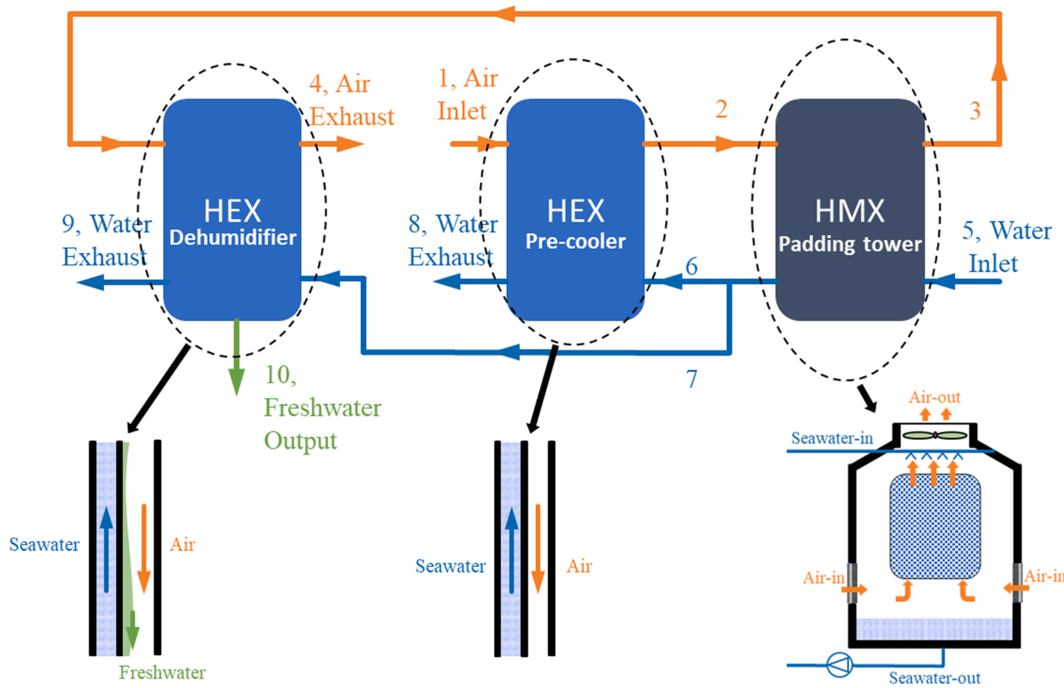

Fig. 8. Desalination system based on IEC chiller system.

(5) Seawater and air are countercurrent heat exchange in HEX or HMX.

Then the model is calculated with equations (22) ~ (30), where the subscript *ideal* represents the case where the minimal heat transfer temperature difference achieves 0 K. The subscripts *air, sw, fw* separately represent the air, seawater, freshwater.

Pre-cooler

$$\omega_{air,in} = \omega_{air,out} \qquad \textit{Mass Conservation} \tag{22}$$

$$\dot{m}_{dryair}\left(h_{air,out} - h_{air,in}\right) = \dot{m}_{sw}\left(h_{sw,in} - h_{sw,out}\right) \qquad \textit{Energy Conservation} \tag{23}$$

$$\varepsilon_{precooler} = \max\left\{\frac{h_{air,out} - h_{air,in}}{h_{air,out,ideal} - h_{air,in}}, \frac{h_{sw,out} - h_{sw,in}}{h_{sw,out,ideal} - h_{sw,in}}\right\} \qquad \textit{Heat Transfer Effectiveness} \tag{24}$$

Dehumidifier

$$\dot{m}_{fw} = \dot{m}_{dryair}\left(\omega_{air,in} - \omega_{air,out}\right) \qquad \textit{Mass Conservation} \tag{25}$$

$$\dot{m}_{dryair}\left(h_{air,out} - h_{air,in}\right) + \dot{m}_{fw}h_{fw} = \dot{m}_{sw}\left(h_{sw,in} - h_{sw,out}\right) \qquad \textit{Energy Conservation} \tag{26}$$

$$\varepsilon_{deh} = \max\left\{\frac{h_{air,out} - h_{air,in}}{h_{air,out,ideal} - h_{air,in}}, \frac{h_{sw,out} - h_{sw,in}}{h_{sw,out,ideal} - h_{sw,in}}\right\} \qquad \textit{Heat Transfer Effectiveness} \tag{27}$$

Padding tower

$$\dot{m}_{sw,out} - \dot{m}_{sw,in} = \dot{m}_{dryair}\left(\omega_{air,in} - \omega_{air,out}\right) \qquad \textit{Mass Conservation} \tag{28}$$

$$\dot{m}_{dryair}\left(h_{air,out} - h_{air,in}\right) = \dot{m}_{sw,in}h_{sw,in} - \dot{m}_{sw,out}h_{sw,out} \qquad \textit{Energy Conservation} \tag{29}$$

$$\varepsilon_{paddingtower} = \max\left\{\frac{h_{air,out} - h_{air,in}}{h_{air,out,ideal} - h_{air,in}}, \frac{h_{sw,out} - h_{sw,in}}{h_{sw,out,ideal} - h_{sw,in}}\right\} \qquad \textit{Heat Transfer Effectiveness} \tag{30}$$

The calculation is based on iteration using Simulink and Matlab R2021a [27].

3.2. Simulation: Results and parameters sensitivity analysis

Unlike traditional HDH system, the IEC chiller desalination doesn't need extra heat source outside, thus, the gained output ratio (GOR) wouldn't be the evaluating parameter. The performance will be evaluated with the daily water product per 1 $m^3{*}s^{-1}$ of air volume flow rate (DWP) [20]. DWP has a unit of [$m^3{*}d^{-1}{*}m^{-3}{*}s$], and DWP equals to 1

Table 2
Inlet parameters of air and seawater.

Serial number	Mass flow rate (dry air or seawater)	Temperature (°C)	Air humidity or seawater concentration
1 (air)	1.144 kg*s^{-1}	30.0	12.0 g*kg^{-1}
5 (seawater)	1.144 kg*s^{-1}	30.0	3.50 %

m^3*d^{-1}*m^{-3}*s represents 1 m^3 of freshwater is condensed in 1 day or 24 h for a system with specific 1 m^3*s^{-1} or 3600 m^3*h^{-1} of air volume flow rate. That means the system's capacity is determined mainly based on the air flow rate, because in terms of specific energy consumption (SEC), it is expectedly almost totally depending on the fans energy consumption to overcome the air resistance. Generally, the water pump consumption can be ignored compare with fans consumption, and there is no other energy consumption in this system. For typical IEC chiller system, the resistance level is at about 300 Pa, corresponding to a 400 W electricity consumption per 1 m^3*s^{-1} of air volume flow rate, considering a motor-mechanical efficiency of 75 %. It is worth mentioning that the air resistance could be optimized to reduce, and according to Pandelidis, et al. [20], their dew point evaporative system is expected to have a resistance of about 15 ~ 20 Pa. In our case, the gas resistance is not taken into consideration and can be seen as constant, thus, SEC is proportional to DWP, and the proportion is only depending on the air resistance. Due to its proportional relationship, in the following analysis only the DWP is selected as the evaluating parameter.

A typical condition is calculated, where the inlet air and inlet seawater parameters are listed in Table 2. The serial numbers correspond to Fig. 8.

The moist air volume flow rate is fixed at 1 m^3*s^{-1}, corresponding to the dry air mass flow rate of 1.144 kg*s^{-1}. The mass flow rate ratio of dry air and seawater is selected as 1:1, and the temperatures are both 30 °C. Besides, the outlet seawater from padding tower splits into two streams. The stream through the dehumidifier portion is called seawater distribution ratio (SDR) here. The SDR in this typical case is selected as 75 %, corresponding to the common value in an IEC chiller. The HEX (pre-cooler and dehumidifier) and HMX (padding tower) heat transfer effectiveness are set to 0.8. In many practical cases, the effectiveness level could achieve 0.8 [6,10], which can be seen as a validation for the simulation.

According to the condition above, the model is simulated, and the results are listed in Table 3. The serial numbers correspond to Fig. 8.

The result represents the water product capacity of this system as 0.00533 kg per 1 m^3 air, corresponding to a DWP of 0.46 m^3*d^{-1}*m^{-3}*s in this condition. The air points are marked in psychrometric chart in Fig. 9. As expected, the inlet air is pre-cooled, humidified, and dehumidified.

Based on the typical condition, keeping the humidity ratio of the inlet air, flow rate and other parameters unchanged, only changing the temperature, the performance is simulated and shown in Fig. 10. Keeping the temperature, flow rate and other parameters unchanged, only changing the air humidity ratio, the performance is simulated and shown in Fig. 11. Keeping the temperature, humidity ratio, flow rate and other parameters unchanged, only changing the heat transfer effectiveness of HEX and HMX, the performance is simulated and shown in Fig. 12. In Figs. 10, 11, the legend *a* and *c* represent previous literature 3-stage and 2-stage Dew Point Desalination (DPD) performance [20]. The legend *b* stands for the performance of the IEC chiller desalination design in this paper, which is right between their 2-stage and 3-stage

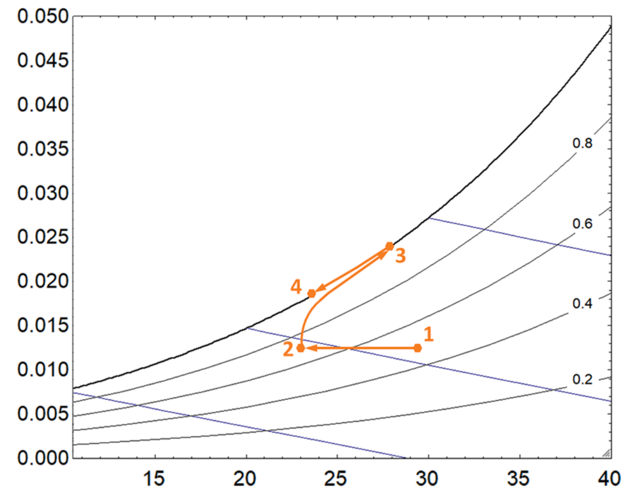

Fig. 9. The air process in psychrometric chart at typical condition.

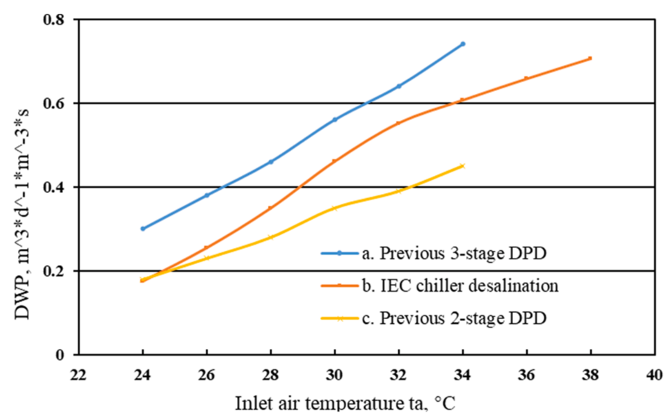

Fig. 10. DWP changing with temperature and comparison with previous results.

Table 3
Simulating results at typical condition.

Serial number	Mass flow rate(dry air or seawater)	Temperature (°C)	Air humidity or seawater concentration
1 (air)	1.144 kg*s^{-1}	30.0	12.0 g*kg^{-1}
2 (air)	1.144 kg*s^{-1}	23.4	12.0 g*kg^{-1}
3 (air)	1.144 kg*s^{-1}	27.9	23.6 g*kg^{-1}
4 (air)	1.144 kg*s^{-1}	24.0	18.9 g*kg^{-1}
5 (seawater)	1.144 kg*s^{-1}	30.0	3.50 %
6 (seawater)	0.283 kg*s^{-1}	21.4	3.54 %
7 (seawater)	0.848 kg*s^{-1}	21.4	3.54 %
8 (seawater)	0.283 kg*s^{-1}	28.3	3.54 %
9 (seawater)	0.848 kg*s^{-1}	26.6	3.54 %
10 (freshwater)	0.00533 kg*s^{-1}	24.0	0

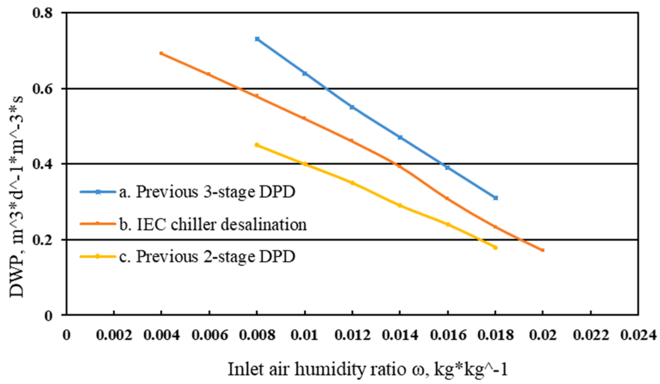

Fig. 11. DWP changing with inlet air humidity ratio and comparison with previous results.

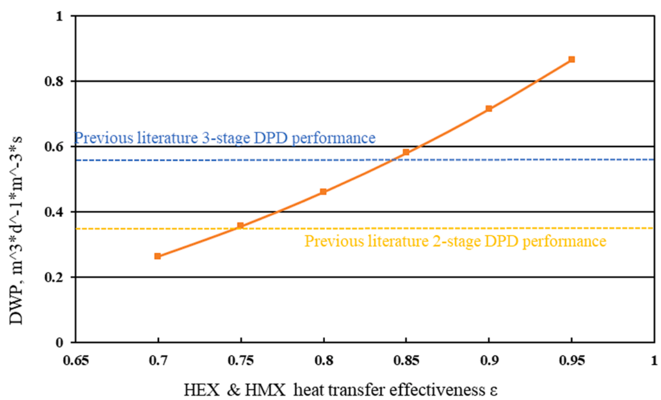

Fig. 12. DWP changing with heat transfer effectiveness and comparison with previous results.

level. According to Figs. 10, 11, the water product increases when the temperature increases and air humidity ratio decreases, which also corresponds to the previous work. In Fig. 12, heat transfer effectiveness is changed, indicating the NTU is changed. Greater heat effectiveness results in greater water product, when the heat effectiveness exceeds 0.84, the performance of this system is better than previous literature 3-stage DPD level. Performance increases 20 %~30 % by per 0.05 of heat transfer effectiveness increase.

Results in Figs. 10 and 11 demonstrate perfectly similar sensitivity of inlet parameters between previous study and this novel process. It is not a coincidence although the two processes are apparently different in

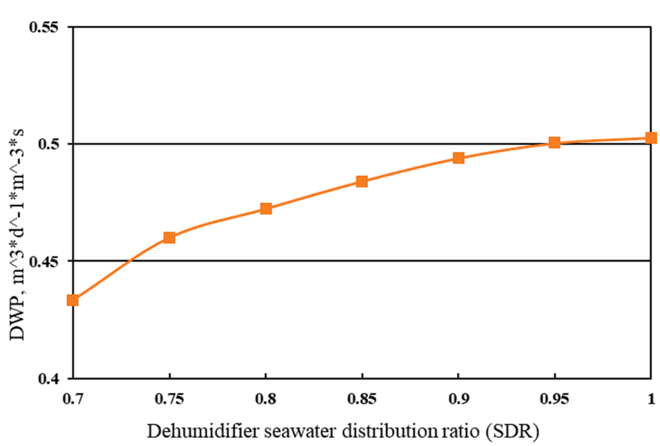

Fig. 13. DWP changing with the dehumidifier water seawater distribution ratio (SDR).

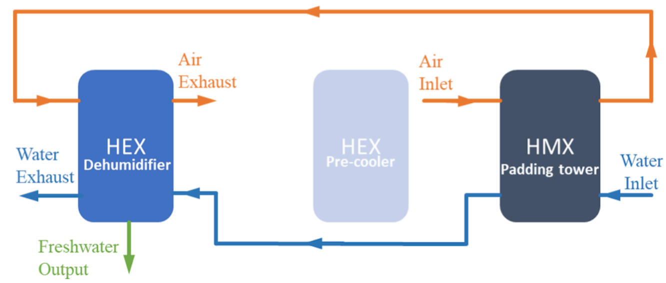

Fig. 14. The system degrades when the pre-cooler is useless.

Fig. 3 and Fig. 8. In fact, the thermodynamics analysis shown in Section 2.4 can explicitly explain the tendency of the parameters sensitivity and the thermodynamics principle behind previous study and this novel process is the same. In a sense, the previous study has become a validation of these results. The truly interesting part is, the performance of this novel process for ε equal to 0.8, which is the usual effectiveness level in practical applications, falls right between the previous literature 2-stage DPD and 3-stage DPD performance. In the previous work [20], 2-stage DPD includes one humidification-dehumidification section while 3-stage DPD includes two. In this novel IEC chiller desalination process, it actually only includes one humidification-dehumidification section. Multi-stage humidification-dehumidification is useful to recover the exergy of the exhaust air and seawater, and this idea can be applied in this novel IEC chiller desalination process in future work.

Seawater distribution ratio (SDR) represents the proportion of the seawater stream through the dehumidifier and has been fixed at 75% in the above simulation. The system performance changes when SDR changes at typical condition, as shown in Fig. 13.

According to Fig. 13, the DWP increases as SDR increases up to 100 %. Pre-cooler is actually useless when SDR achieves 100 %. The system degrades into an open-cycle HDH system, but without an extra heat resource, as shown in Fig. 14. On the other hand, IEC has dew point cooling potential only when the air is pre-cooled. If pre-cooler is useless in this condition, the desalination system also has nothing to do with the dew point under these circumstances.

The crucial parameter is the inlet seawater temperature. At typical condition, the inlet air and water temperature are both 30 °C, but if the temperature of seawater changes while that of air remains 30 °C, new performance changing characteristics by SDR appear as shown in Fig. 15. Each larger marker on the curve represents the optimal SDR ratio.

According to Fig. 15, the inlet seawater temperature has a great influence on water product. The freshwater product halves when inlet seawater temperature decreases by 4 °C. And as the inlet seawater temperature decreases, the optimal SDR decreases. It indicates the pre-cooler has certain effect, which is related to dew point evaporative

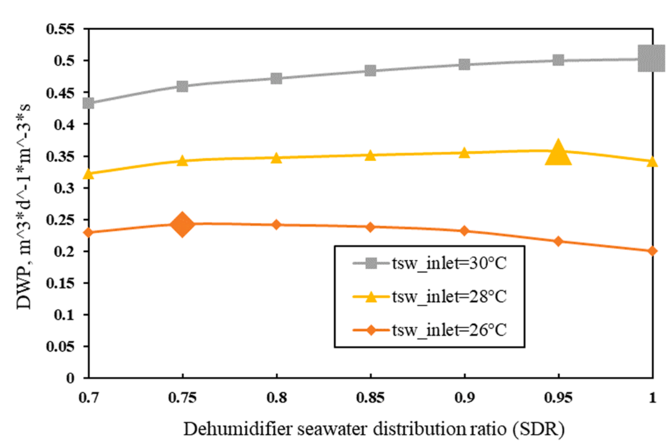

Fig. 15. DWP changing with SDR under different inlet seawater temperatures.

cooling. In fact, the temperatures of air and seawater are different in most time, since the air temperature fluctuates a lot by seasons and seawater temperature fluctuates little. In the hot season, the water temperature usually is lower than that of the air. Thus, the discussion on inlet seawater temperature is important in desalination based on air-seawater system. Besides, due to IEC chiller is similar to regenerative IEC, and the previous dew point desalination system (DPD) literature is partly based on regenerative IEC, the DPD system may face similar problem when the inlet seawater temperature changes, since Pandelidis, et al. [20] did not discuss much about seawater temperature effects in the previous literature.

The influence of inlet seawater temperature and SDR highlights the difference between HDH and IEC chiller desalination. In conventional HDH, there is extra heat resource, and the seawater acts as cooling resource. But in IEC chiller desalination system, the sensible heat of the air and the seawater acts as heat resource, and the cooling resource is provided by the air-seawater evaporative cooling. Evaporative cooling temperature depends on the air, and the limit is the dew point for an IEC configuration. But without air pre-cooled, the evaporative cooling temperature is usually higher than wet bulb. Thus, when the inlet seawater temperature decreases, on one hand the heat resource decreases so the water product decreases, on the other hand the temperature difference between inlet seawater temperature and wet bulb decreases resulting in that pre-cooler need to reflect its effect and the optimal SDR decreases.

3.3. Discussion

According to the theoretical limit discussed by Section 2, under the typical condition, the water product limit is 0.138 kg for both 1 kg of air (@30 °C, rh = 45 %) and 1 kg of seawater (@30 °C, x = 3.5 %), corresponding to a DWP of 13.87 $m^3{*}d^{-1}{*}m^{-3}{*}s$. On the other hand, the simulated performance of our designed IEC chiller desalination system under typical condition is 0.503 $m^3{*}d^{-1}{*}m^{-3}{*}s$. From the perspective of water product, the reversible efficiency is only 3.6 %. Although the air-seawater is free in reality, considering the air resistance discussed in Section 3.1, the DWP of 0.503 $m^3{*}d^{-1}{*}m^{-3}{*}s$ corresponds to the SEC of about 19.1 $kWh{*}m^{-3}$ when the gas resistance level is 300 Pa, which still costs a lot. Improved design of heat and mass transfer structures with better fluid flow is possible and can effectively enhance this result. For some regenerative IEC cases, the gas resistance is below 50 Pa, which could lead to a reduction in energy consumption by 1/6. That could be a level of highly efficient. Thus, reducing air resistance can significantly improve energy efficiency.

Besides the gas resistance, there are several optimized strategies to increase DWP based on irreversible loss distribution analysis.

Firstly, the loss occurs because the heat transfer effectiveness is lower than 1, which has been discussed in Section 3.1. According to the simulation, the performance improves by 20 ~ 30 % per 0.05 increase in heat transfer effectiveness.

The loss also occurs when the heat capacity flow rates of two sides are different, and this can't be avoided even heat transfer effectiveness achieves 1. Miller and Lienhard [28] proposed extraction process in HDH system to minimize the entropy generation. McGovern, et al. [29] and Narayan, et al. [30] furtherly discussed and demonstrate that multi-section and extraction process in HDH system could decrease the entropy generation and obtain higher gained output ratio. Xie and Jiang [10,26] also emphasized the importance of heat capacity flow rate match in IEC systems. Thus, it is also recommended to use these ideas in IEC chiller desalination system.

Besides, there still remains some work potential for outlet air and seawater, so adding another stage of humidification-dehumidification of the outlet air and seawater could increase fresh water product. According to Section 3.2, the performance of this novel process at typical condition falls right between the 2-stage DPD and 3-stage DPD performance in the study of Pandelidis, et al. [20]. In fact, the 3-stage DPD system is based on the multi-stage principle and one more humidification-dehumidification section is added to increase fresh water product. This multi-stage method can also be used for IEC chiller desalination system in this paper to achieve higher performance.

For applications, another crucial point to consider is the climate conditions. Particularly, air temperature is usually independent of seawater temperature, and according to the simulation results obtained in this paper, the two factors both influence system performance. This implies that, even within the same region, the performance in different seasons cannot be predicted solely using the air temperature index; it also needs to take into account the seawater temperature. These two parameters typically vary independently with the changing seasons. Generally, a dry and hot climate is more favorable for this water production system, typically found in low-latitude regions where monsoons blow from land to the sea. Despite these limitations, the concept of water production from air-sea systems holds significant potential for improvement. Particularly, the exergy of non-equilibrium air-seawater system is abundant and virtually limitless, and theoretical calculations in the Section 2 demonstrate substantial energy under specific circumstances. If effectively applied in the field of seawater desalination, it could lead to substantial economic benefits and a reduction in carbon emissions.

4. Conclusion

This paper explores the feasibility of seawater desalination using a non-equilibrium air-seawater system and presents the design of an IEC chiller desalination system. The key findings and conclusions of this study can be summarized as follows:

(1) The paper calculate the theoretical air-seawater system work capacity and desalination potential based on thermodynamics. For a system include 1 kg of air (@30 °C, rh = 45 %) and 1 kg of seawater (@30 °C, x = 3.5 %), it can be determined that this system could perform a maximum work of 0.419 kJ, and has a water product potential of 0.138 kg. The work capacity and desalination potential increase while the relative humidity decreases or the temperature of air and water increases.

(2) To conduct the thermodynamics calculations, the concepts of system exergy and reversible transition are introduced to analyze the work capacity and water product capacity of the air-seawater system. Moist air exergy is generally used to describe the work capacity of air–water system and is written in textbook, however, the calculation of moist air exergy is based on the reference, which implies infinite amount of water at reference point. The concepts of system exergy and reversible transition are proposed to handle situations where the flow rate ratio of seawater to air is finite. System exergy represents the maximum work capacity of a non-equilibrium system for an adiabatic and isobaric process. Reversible transition of a non-equilibrium air-seawater system is proposed to calculate its maximum desalination capacity by assuming a thermal equilibrium air-seawater-freshwater final state. These two concepts could not only help to understand IEC and HDH processes which include air–water systems, but also provide insights into the field of thermodynamic analysis.

(3) An IEC chiller desalination system is designed, modeled, and simulated. The system only includes common padding towers, pre-coolers, and dehumidifiers. At typical condition, where the temperature of air and seawater is 30 °C; the relative humidity ratio 45 %; the concentration of seawater is 3.5 %; the mass flow rate ratio of air to seawater is 1:1 and the heat transfer effectiveness is set to a practical value of 0.8, the system performance is simulated, and a daily water product capacity (DWP) of 0.503 $m^3{*}d^{-1}{*}m^{-3}{*}s$ is obtained, which means 0.503 m^3 of freshwater is condensed in 1 day or 24 h for a system with specific 1 $m^3{*}s^{-1}$ or 3600 $m^3{*}h^{-1}$ of air volume flow rate. The sensitivity analysis of parameters such as inlet temperature and air humidity shows

consistent trends with previous findings. The influence of the inlet seawater temperature, which has not been discussed previously, is investigated. It is simulated that a decrease in the inlet seawater temperature significantly reduces the water product capacity and affects the optimal seawater distribution ratio (SDR) in the IEC chiller desalination system. This effect is attributed to the fact that seawater serves as a heat source in this system rather than as a cooling source in a common HDH system. This effect implies that the performance in different seasons is determined not only by the air temperature index but also the seawater temperature. These two parameters typically vary independently with the changing seasons.

(4) It is expected that the energy consumption of the IEC chiller desalination system is nearly all from the gas resistance, or air fan consumption. Although the typical gas resistance level of an IEC chiller is about 300 Pa, if the gas resistance of this system is reduced to below 50 Pa, the specific water product energy consumption could achieve 3.2 kWh*m^{-3}. Besides, comments of irreversible loss in the system are given, and several optimization strategies are proposed. These strategies include improving heat transfer effectiveness, incorporating multi-section and extraction processes, and adding additional stages of humidification-dehumidification to enhance the freshwater production. These strategies may improve the performance in further study.

In summary, this paper explores the seawater desalination potential of the air-seawater system and presents the design of an IEC chiller desalination system based on this concept. The results show that there is still significant room for improvement, since the simulated practical water product capacity is equal to only 3.6 % of the theoretical reversible limit. How to reduce gas resistance and how to optimize the process to reduce entropy production need to be considered to further investigate the feasibility. Overall, considering the exergy inherent in non-equilibrium air-seawater systems is abundant, the concept of desalination based on non-equilibrium air-seawater system still holds promise as it has great potential to yield economic benefits and reduce carbon emissions.

Declaration of Competing Interest

The authors declare that they have no known competing financial interests or personal relationships that could have appeared to influence the work reported in this paper.

Data availability

Data will be made available on request.

Acknowledgement

The authors gratefully acknowledge the support from National Key Research and Development Program of China (Key Projects of International Cooperation in Science and Technology Innovation) (Grant number 2019YFE0102700), National Key Research and Development Program of China (Grant number 2022YFC3802403), and Tsinghua University Initiative Scientific Research Program (Grant number 20221080079).

References

[1] M.A. Abdelkareem, M. El Haj Assad, E.T. Sayed, B. Soudan, Recent progress in the use of renewable energy sources to power water desalination plants, Desalination 435 (2018) 97–113.

[2] A. Ali, V.R. Singh, S. Maheshwari, S. Chaurey, S. Lodhi, Solar desalination using humidification dehumidification process, Mater. Today:. Proc. 62 (2022) 6900–6904.

[3] T.M. Khass, R.H. Mohammed, N.A.A. Qasem, S.M. Zubair, "Different configurations of humidification-dehumidification desalination systems: Thermal and economic assessment." Energy Convers. Manage. 2022, 258.

[4] H. Xu, S. Jiang, M.X. Xie, T. Jia, Y.J. Dai, Technical improvements and perspectives on humidification-dehumidification desalination — A review, Desalination 541 (2022).

[5] I. Hussain, F. Bibi, S.A. Bhat, U. Sajjad, M. Sultan, H.M. Ali, M.W. Azam, S. K. Kaushal, S. Hussain, W.-M. Yan, Evaluating the parameters affecting the direct and indirect evaporative cooling systems, Eng. Anal. Bound. Elem. 145 (2022) 211–223.

[6] Y. Jing, C. Zhao, X. Xie, Y. Jiang, Optimization and performance analysis of water-mediated series indirect evaporative chillers: Experimental and simulated investigation, Energy Convers. Manage. 2022, 268.

[7] K. Yang, X. Hao, Y. Lin, Q. Xing, H. Tan, J. Hu, X. Liu, An integrated system of water-cooled VRF and indirect evaporative chiller and its energy saving potential, Appl. Therm. Eng. 194 (2021).

[8] R.H. Mohammed, M. El-Morsi, O. Abdelaziz, "Indirect evaporative cooling for buildings: A comprehensive patents review." Journal of Building, Engineering 50 (2022).

[9] H. Yang, W. Shi, Y. Chen, Y. Min, Research development of indirect evaporative cooling technology: An updated review, Renew. Sustain. Energy Rev. 145 (2021).

[10] Y. Jiang, X. Xie, Theoretical and testing performance of an innovative indirect evaporative chiller, Sol. Energy 84 (12) (2010) 2041–2055.

[11] J. Chu, W. Xu, X. Huang, Z. Geng, J. Xuan, Study on optimization of indirect-direct evaporative chiller for producing cold water in hot and dry areas, Renew. Energy 181 (2022) 898–913.

[12] Y. Yang, C. Ren, C. Yang, M. Tu, B. Luo, J. Fu, Energy and exergy performance comparison of conventional, dew point and new external-cooling indirect evaporative coolers. Energy Conversion and Management 230, 2021.

[13] X. Xie, Y. Jiang, Comparison of two kinds of indirect evaporative cooling system: to produce cold water and to produce cooling air, Procedia Eng. 121 (2015) 881–890.

[14] Y. Jing, X. Xie, Y. Jiang, Performance comparison and suitable climatic zones of three water-mediated evaporative cooling technologies. Energy Conversion and Management 277, 2023.

[15] A.E. Kabeel, M. Abdelgaied, M.B. Feddaoui, Hybrid system of an indirect evaporative air cooler and HDH desalination system assisted by solar energy for remote areas, Desalination 439 (2018) 162–167.

[16] Q. Chen, M. Burhan, M.W. Shahzad, D. Ybyraiymkul, F.H. Akhtar, K.C. Ng, Simultaneous production of cooling and freshwater by an integrated indirect evaporative cooling and humidification-dehumidification desalination cycle. Energy Conversion and Management 221, 2020.

[17] R. Tariq, N.A. Sheikh, J. Xamán, A. Bassam, An innovative air saturator for humidification-dehumidification desalination application, Appl. Energy 228 (2018) 789–807.

[18] M.A. Aziz, J. Lin, F. Mikšík, T. Miyazaki, K. Thu, The second law analysis of a humidification-dehumidification desalination system using M-cycle. Sustainable Energy Technologies and Assessments 52, 2022.

[19] Rocchetti, A. and L. Socci (2022). "Theoretical and numerical assessment of an enhanced Humidification-Dehumidification desalination system based on Indirect Evaporative cooling and Vapour Compression Refrigeration." Applied Thermal Engineering 208.

[20] D. Pandelidis, A. Cichoń, A. Pacak, P. Drąg, M. Drąg, W. Worek, S. Cetin, Water desalination through the dewpoint evaporative system, Energy Convers. Manage., 2021, 229.

[21] Advanced Engineering Thermodynamics: by Adrian Bejan, Wiley, New York, 1988. ISBN 0-471-61747-4.

[22] W. Li, Y. Li, W. Shi, J. Lu, Energy and exergy study on indirect evaporative cooler used in exhaust air heat recovery, Energy (2021) 235.

[23] NIST Reference Fluid Thermodynamic and Transport Properties Database (REFPROP), available at https://www.nist.gov/srd/refprop.

[24] K.G. Nayar, M.H. Sharqawy, L.D. Banchik, J. H. Lienhard V,, Thermophysical properties of seawater: A review and new correlations that include pressure dependence, Desalination 390 (2016) 1–24.

[25] S.A. Klein, Engineering Equation Solver. (2010). Software available at http://www. fchartsoftware.com/ees/.

[26] X. Xie, "Research on Indirect Evaporative Cooling Air Conditioning System," Ph.D. thesis, Dept. Building Science and Technology, Chinese, Tsinghua Univ., Beijing, China, 2008.

[27] The Math Works, Inc, MATLAB, Version, 2020.

[28] J.A. Miller, J. H. Lienhard V,, Impact of extraction on a humidification–dehumidification desalination system, Desalination 313 (2013) 87–96.

[29] R.K. McGovern, G.P. Thiel, G. Prakash Narayan, S.M. Zubair, J.H. Lienhard, Performance limits of zero and single extraction humidification-dehumidification desalination systems, Appl. Energy 102 (2013) 1081–1090.

[30] G.P. Narayan, K.M. Chehayeb, R.K. McGovern, G.P. Thiel, S.M. Zubair, J. H. Lienhard V,, Thermodynamic balancing of the humidification dehumidification desalination system by mass extraction and injection, Int. J. Heat Mass Transf. 57 (2) (2013) 756–770.